Research Square

Preprints are preliminary reports that have not undergone peer review.
They should not be considered conclusive, used to inform clinical practice,
or referenced by the media as validated information.

InSilico-K: a drug-agnostic digital twin showing that molecular weight, not molecular target, governs biologic delivery and its telmisartan-mediated rescue in non-small cell lung cancer

Junichi Shimada

shimajun@koto.kpu-m.ac.jp

Kyoto Prefctural University of Medicine https://orcid.org/0000-0002-5288-5539

Research Article

Keywords: InSilico-K, InSilico-pCR, non-small cell lung cancer, interstitial fluid pressure, telmisartan, angiotensin receptor blocker, antibody–drug conjugate, digital twin, drug delivery, surgical de-escalation

Posted Date: November 6th, 2026

DOI: https://doi.org/10.21203/rs.3.rs-10224699/v3

License: This work is licensed under a Creative Commons Attribution 4.0 International License.
Read Full License

Additional Declarations: The authors declare no competing interests.

InSilico-K: a drug-agnostic digital twin showing that molecular weight, not molecular target, governs biologic delivery and its telmisartan-mediated rescue in non-small cell lung cancer

Junichi Shimada, MD, PhD

Graduate School of Nursing for Health Care Science, Kyoto Prefectural University of Medicine, Kyoto, Japan

Correspondence: shimajun@koto.kpu-m.ac.jp

ORCID 0000-0002-5288-5539

Abstract

Background. Modern non-small cell lung cancer (NSCLC) therapy is increasingly built from immunoglobulin-scale biologics—bispecific antibodies, antibody–drug conjugates (ADCs), checkpoint inhibitors and anti-angiogenic antibodies—all clustered near ~145–153 kDa, roughly 300-fold heavier than the tyrosine kinase inhibitors (TKIs) they accompany. We tested the hypothesis that elevated tumour interstitial fluid pressure (IFP) throttles this entire weight-class identically, and that a single safe antihypertensive, telmisartan, could decompress it universally. This work extends our earlier single-agent digital twin of amivantamab (Research Square, 2025) to a drug-agnostic framework.

Methods. We built an open, deterministic digital-twin engine (InSilico-K) in which molecular weight is the only drug-specific input. Baseline IFP is estimated from CT-derived tumour volume, mean arterial pressure and serum albumin; telmisartan decompresses it by first-order decay; effective tissue diffusion combines an IFP penalty (applied only to macromolecules) with steric exclusion by molecular weight; cumulative receptor occupancy is mapped to a response probability we term the in-silico pathological complete response (InSilico-pCR). Seventeen approved or late-stage agents (nine macromolecular, eight small-molecule) were catalogued and simulated for a representative virtual patient.

Results. Current agents form a bimodal molecular-weight landscape with an empty middle: nine macromolecular agents at ~145,000–153,000 Da and eight TKIs at ~406–561 Da, separated ~315-fold. For the virtual patient (tumour volume 8.0 cm^3, mean arterial pressure 100 mmHg, serum albumin 3.8 g/dL) baseline IFP was 24.0 mmHg and decayed to 7.8 mmHg by Day 7 under modelled telmisartan. Effective-diffusion trajectories for three different macromolecular classes were superimposable, each accelerating ~5.9-fold, while the small molecule osimertinib was unchanged. Modelled InSilico-pCR rose from ~31–36% under standard care to ~89–93% under telmisartan across all nine macromolecular agents (reference agent 34.2% → 91.5%); small molecules derived no benefit.

Conclusions. In silico, IFP decompression behaves as a property of a molecular-weight class rather than of any single drug or target. Because the principle is tied to molecular weight, it does not expire when first-line therapy changes, motivates a cardiology–oncology co-prescribing strategy, and—if verified—supports surgical de-escalation, which we formalise as InSilico-Guided Minimal Resection (IGMR). We outline a minimal, falsifiable window-of-opportunity study to test the framework in tissue.

Keywords: InSilico-K; InSilico-pCR; non-small cell lung cancer; interstitial fluid pressure; telmisartan; angiotensin receptor blocker; antibody–drug conjugate; digital twin; drug delivery; surgical de-escalation.

1. Introduction

Precision therapy for non-small cell lung cancer (NSCLC) is being rebuilt out of biologics. The bispecific antibody amivantamab combined with the tyrosine kinase inhibitor (TKI) lazertinib is now established in advanced EGFR-mutated disease [1,2], with a subsequent overall-survival advantage over osimertinib [3]; antibody–drug conjugates (ADCs) against TROP2 [4], HER2 [5] and HER3 [6] are reshaping later lines [7]; and checkpoint inhibitors and anti-angiogenic antibodies complete an ecosystem dominated by large molecules.

Our earlier work modelled a single such agent—the 148-kDa amivantamab—as the macromolecule whose tumour delivery is throttled by elevated interstitial fluid pressure (IFP), and mapped its predicted pathological response in an open digital-twin platform for neoadjuvant optimisation and surgical de-escalation [8]. Here we make a broader claim. Amivantamab is not special; it is representative. Every IgG-based biologic in thoracic oncology sits within a narrow ~145–153 kDa band (Table 1) and therefore confronts the same convective barrier. The axis that decides whether a drug reaches the tumour core is molecular weight, not molecular target.

Elevated IFP restricts convection and diffusion of macromolecules while sparing small molecules. Angiotensin inhibition decompresses tumour vasculature and enhances drug delivery [9]; telmisartan, an angiotensin II type 1 receptor blocker, specifically stabilises tumour perfusion and reduces hypoxia [10], consistent with the mechanopathology of the tumour microenvironment [11]. We reasoned that if a safe oral antihypertensive can decompress that barrier for one macromolecule, it should do so for the whole weight-class. To make this testable rather than rhetorical, we cast it as an open, drug-agnostic digital twin—an approach now widely surveyed across health [12]—in which molecular weight is the only drug-specific input, so that new agents—including biologics not yet approved—are added as data, not code. This paper reports the engine, the cross-class simulation results, and a minimal design to falsify the hypothesis in tissue.

2. Methods

2.1 The InSilico-K digital-twin engine

InSilico-K is a deterministic, three-layer engine (Box 1). Molecular weight (Da) is the only drug-specific input. Baseline IFP is estimated from a non-invasive triad—CT-derived tumour volume, mean arterial pressure (MAP) and serum albumin—and is then decompressed by telmisartan as first-order decay. Effective tissue diffusion combines a pressure penalty, applied only to macromolecules via a binary flag, with steric exclusion by molecular weight. Receptor occupancy integrates target affinity, effective diffusion, the albumin-dependent free fraction and free drug concentration; the time-integral of occupancy maps to a response probability. Structural target-affinity priors were informed by contemporary biomolecular structure prediction [13]; the response mapping draws on classical tumour-growth formulations [14], the Norton–Simon principle relating tumour size to therapeutic sensitivity [15], and evolutionary models of response to targeted

combination therapy [16].

2.2 Outcome mapping: InSilico-pCR

The engine converts cumulative receptor occupancy into a continuous probability of pathological complete response, which we designate the in-silico pathological complete response (InSilico-pCR) to distinguish it from the wet-lab, tissue-confirmed pathological complete response it is intended to predict. InSilico-pCR is a model output, not a measured endpoint; its role in this study is comparative—contrasting standard care with telmisartan across agents—rather than absolute.

2.3 Drug database

Seventeen agents relevant to thoracic oncology were catalogued (Tables 1 and 2): nine macromolecular agents across four mechanistic classes (bispecific antibody, ADC, checkpoint inhibitor, anti-angiogenic antibody) and eight small-molecule TKIs. Antibody and ADC molecular weights were treated as an approximate intact-antibody-scale band (~145–153 kDa); TKI weights are exact formula masses. Each agent enters the engine solely through its molecular-weight value and, where relevant, a class flag.

2.4 Virtual patient and simulation protocol

A representative virtual patient was defined (tumour volume 8.0 cm^3, MAP 100 mmHg, serum albumin 3.8 g/dL). Two arms were simulated: standard care (no decompression) and modelled oral telmisartan once daily. IFP, effective diffusion and InSilico-pCR were computed over a 28-day window for every catalogued agent, with IFP and effective-diffusion trajectories additionally reported at Day 7 as an early decompression checkpoint. To probe class-independence, three macromolecules from three different classes (amivantamab, datopotamab deruxtecan, pembrolizumab) and one small molecule (osimertinib) were compared head-to-head.

2.5 Calibration and coefficients

Coefficients are stylised values pooled from the literature and calibrated by sensitivity analysis so that the reference macromolecule reproduces a physiologically plausible regime (baseline IFP 24 mmHg; Day-7 IFP 7.8 mmHg as an interim decompression checkpoint; ~5.9-fold transport gain; InSilico-pCR 34.2% → 91.5% integrated over the full 28-day window); they were not fitted to patient-level data. All equations, the derivation, coefficient values and runnable code are provided (Box 1; Supplementary Information / repository).

2.6 Ethics

This is an entirely in-silico modelling study using no human subjects, no patient-level data and no identifiable information; ethics approval was therefore not required. The prospective validation design proposed in Section 4 would require institutional review board approval before any patient enrolment.

Box 1 | The InSilico-K model in brief

Molecular weight (Da) is the only drug-specific input. Baseline IFP is estimated from CT-derived tumour volume, mean arterial pressure (MAP) and serum albumin, then decompressed by telmisartan as first-order decay:

$$\text{Baseline_IFP} = k1 \cdot \text{Volume} + k2 \cdot \text{MAP} - k3 \cdot \text{Albumin} \quad (1)$$

$$\text{Dynamic_IFP}(t) = \text{Baseline_IFP} \cdot \exp(-k_\text{telmi} \cdot t) \quad (2)$$

Effective tissue diffusion combines a pressure penalty (applied only to macromolecules via a 1/0 flag) with steric exclusion by molecular weight:

$$\text{Eff_Diff}(t) = D0 \cdot \exp(-k4 \cdot \text{Dynamic_IFP}(t) \cdot \text{flag}) \cdot (1 - \text{MW}/\text{MW_cut}) \quad (3)$$

Receptor occupancy integrates affinity, diffusion, free fraction and free drug; its time-integral maps to a response probability:

$$\text{Occupancy}(t) = \text{Affinity} \cdot \text{Eff_Diff}(t) \cdot f_u(\text{Albumin}) \cdot C_{free}(t) \quad (4)$$

where the free-drug fraction $f_u(\text{Albumin}) = \text{clip}(1 - 0.08 \cdot \text{Albumin}, 0.3, 1.0)$, and, in the absence of agent-specific structural data, base Affinity and C_free were each set to 1.0 (dimensionless reference values), leaving f_u(Albumin) as the sole active term in Eq. 4 for the present calibration.

$$\text{Response} = 1 - \exp(-\alpha \cdot \int \text{Occupancy}(t)\, dt) \quad (5)$$

Coefficients (k1=1.10, k2=0.30, k3=3.90, k_telmi=0.16, k4=0.0889, MW_cut=200,000 Da, α=0.69637) are calibrated so the reference macromolecule reproduces the regime baseline IFP 24 mmHg, Day-7 IFP 7.8 mmHg (interim checkpoint), ~5.9-fold transport gain, InSilico-pCR 34.2% → 91.5% integrated over a 28-day window.

3. Results

3.1 A ~300-fold molecular-weight cliff, not a spectrum

Cataloguing current agents revealed a bimodal landscape with an empty middle (Fig. 1). Nine macromolecular agents across four mechanistic classes clustered at ~145,000–153,000 Da; eight small-molecule TKIs fell at ~406–561 Da (Tables 1, 2). The mean separation was roughly 315-fold, with no drugs occupying the two orders of magnitude between. This physical discontinuity—not pharmacological classification—is what a delivery strategy can exploit: the same barrier confronts every member of the upper cluster.

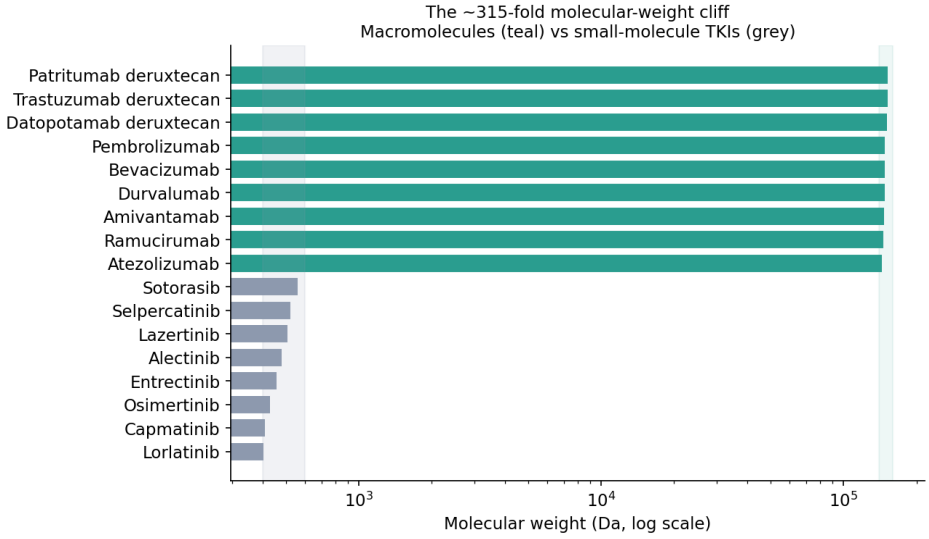


Fig. 1 | The molecular-weight cliff. Macromolecular agents (teal) and small-molecule TKIs (grey) on a

logarithmic scale, separated by ~315-fold with no intermediate occupancy.

3.2 The engine

The same equations apply unchanged to bispecifics, ADCs, checkpoint inhibitors and anti-angiogenic antibodies; new agents are added as data (a single molecular-weight value), not code (Fig. 2).

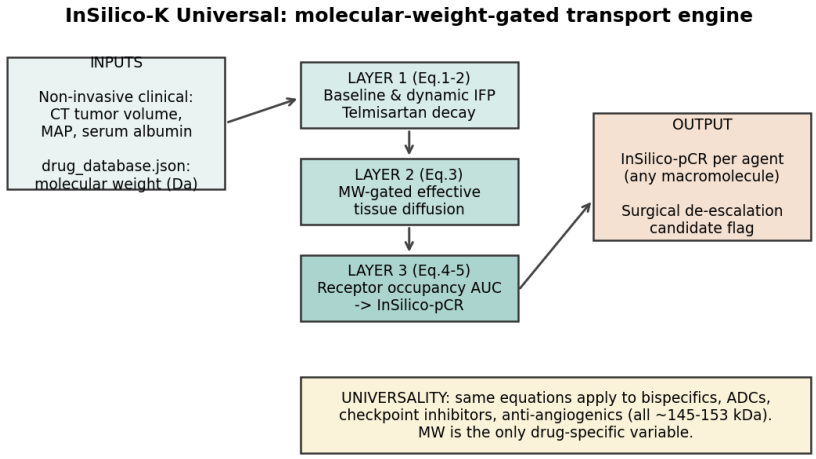


Fig. 2 | The InSilico-K engine. Non-invasive inputs and a single molecular-weight value per drug feed three layers, yielding a per-agent response estimate. The same equations apply unchanged to bispecifics, ADCs, checkpoint inhibitors and anti-angiogenic antibodies.

3.3 IFP dynamics under telmisartan

For the representative virtual patient, baseline IFP was 24.0 mmHg. Under standard care it remained chronically elevated, confining all macromolecules to the tumour periphery; modelled daily telmisartan produced exponential decay to 7.8 mmHg by Day 7, crossing the capillary filtration threshold (Fig. 3a).

3.4 Class-independent transport rescue

The resulting transport rescue was essentially independent of which macromolecule was modelled: amivantamab, datopotamab deruxtecan and pembrolizumab—three different mechanistic classes—showed superimposable effective-diffusion trajectories, each accelerating ~5.9-fold, while the small-molecule osimertinib was unchanged (Fig. 3b).

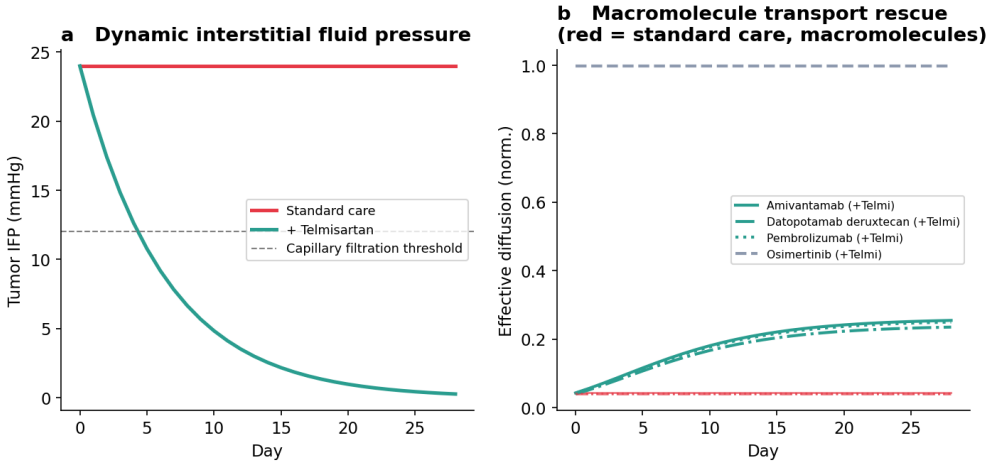


Fig. 3 | a, Dynamic IFP under standard care (red) versus telmisartan (teal), crossing the capillary filtration threshold by Day 7. b, Effective diffusion: macromolecules from three classes (teal) rise nearly identically under telmisartan from the suppressed standard-care baseline (red), while the small-molecule osimertinib (grey dashed) is transport-independent.

3.5 Convergent response-probability gain

At the outcome level the convergence held: modelled InSilico-pCR rose from ~31–36% under standard care to ~89–93% under telmisartan across all nine macromolecular agents, with the reference agent shifting from 34.2% to 91.5% (Fig. 4). The ~57-point gain was nearly uniform across mechanistic classes. Small molecules, being transport-insensitive, derived no benefit. The central point is qualitative as much as quantitative: IFP decompression behaves as a property of a weight-class, not of any one drug.

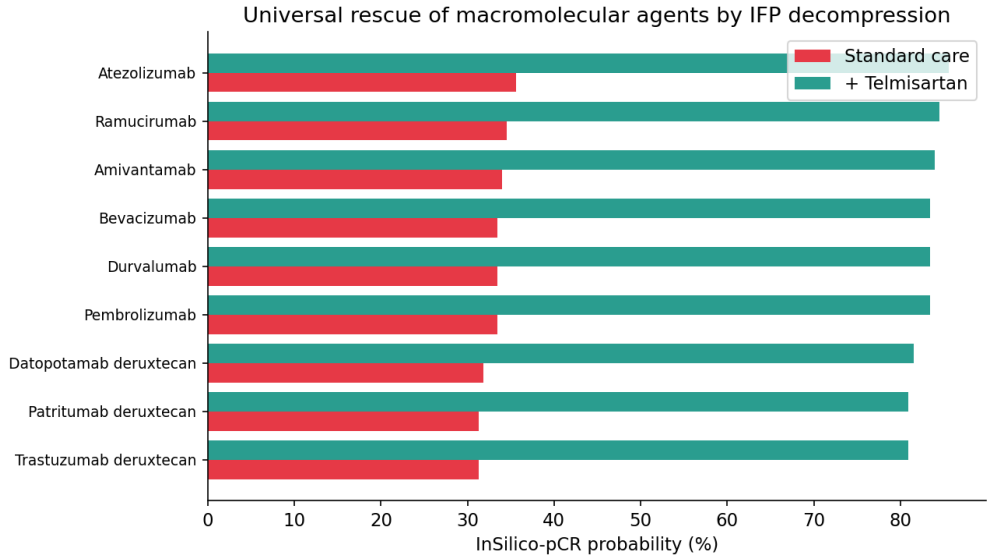


Fig. 4 | Modelled response probability (InSilico-pCR) for nine macromolecular agents under standard care (red) versus telmisartan (teal). The ~57-point gain is nearly uniform across mechanistic classes.

4. Discussion

In silico, tumour IFP decompression behaves as a property of a molecular-weight class rather than of any single drug or target. Because every IgG-scale biologic in thoracic oncology occupies the same narrow ~145–153 kDa band, a strategy that opens the tumour core for one of them is predicted to open it for all. The implication that most motivates this analysis is cross-disciplinary.

4.1 A bridge between cardiology and oncology

Hypertension belongs to the cardiologist; antibody oncology to the medical oncologist; the two rarely co-prescribe with shared intent. Yet a single inexpensive, globally available angiotensin receptor blocker may improve the intratumoral delivery of the most sophisticated cancer biologics. We therefore frame telmisartan not as a new drug but as a bridge—an invitation for both specialties to test together whether a pill already in millions of medicine cabinets can open the tumour core for an entire generation of drugs. Cardiology itself offers a precedent for disciplined de-escalation and device refinement, from drug-eluting stents [17] to anatomy-guided choice between percutaneous and surgical revascularisation [18]; an analogous, physiology-guided partnership could refine how biologics reach the tumour. Because the principle is tied to molecular weight rather than to any single agent or target, it does not expire when first-line therapy changes.

4.2 Surgical de-escalation and InSilico-Guided Minimal Resection (IGMR)

A universal delivery principle also strengthens the case for surgical de-escalation. Phase III non-inferiority trials have established the oncological safety of sublobar resection for small peripheral tumours [19,20], overturning the historical standard set decades earlier by the Lung Cancer Study Group [21], and ACOSOG Z0030 showed no survival benefit from complete mediastinal lymphadenectomy over sampling in node-negative disease [22]. Neoadjuvant targeted therapy can already drive deep pathological responses in resectable EGFR-mutated disease [23], so if pre-operative biologic therapy—universally delivered via IFP decompression—can achieve computationally anticipated, and ultimately tissue-verified, pathological clearance (InSilico-pCR), physical surgery could be repurposed from primary curative modality to a minimalist adjunct.

We formalise this as **InSilico-Guided Minimal Resection (IGMR)**: resection deliberately limited to residual macroscopic disease, guided by the engine's per-patient eradication prediction, after systemic molecular eradication. IGMR is introduced here as a new term to avoid ambiguity. The phrase "adjuvant surgery" has been applied by Yoshida and colleagues to radical (R0-intent) resection after conversion chemotherapy in stage IV gastric cancer [24]—an essentially opposite intent, in which surgery is the decisive curative act. IGMR inverts that logic: systemic therapy is primary and curative, and surgery is the minimal, confirmatory adjunct. Using a distinct term prevents the two paradigms from being conflated.

4.3 A minimal, falsifiable validation design

The hypothesis can be falsified by a small, single-institution, investigator-initiated window-of-opportunity (Phase 0) study requiring no new drug and no industry sponsorship. We envisage 12–20 patients with resectable early-stage NSCLC eligible for a macromolecular agent. After a single neoadjuvant dose of that agent, patients receive oral telmisartan 40 mg daily for 7–14 days until operation, with routine blood-pressure monitoring as the only added safety requirement.

The pre-specified primary endpoint is the intratumoral drug-concentration gradient—tumour core

versus periphery—quantified on the resected specimen by LC-MS/MS or spatially resolved mass-spectrometry imaging, using each tumour's own rim as an internal control and comparing the measured gradient against the patient-specific model prediction. Secondary endpoints include change in IFP (intraoperative wick-in-needle or a dynamic contrast-enhanced MRI perfusion surrogate), hypoxia and collagen markers, and tolerability. A randomised telmisartan-versus-observation allocation would strengthen inference but is not essential for a first signal. A single positive gradient curve—predicted in silico, confirmed in tissue—would convert this framework from hypothesis to evidence and justify a larger efficacy trial.

4.4 Limitations

This is a hypothesis-generating modelling study, not a validated instrument. The engine is a deterministic abstraction; its coefficients are stylised values pooled from literature and calibrated by sensitivity analysis, not fitted to patient-level data. During code archiving, an inconsistency between the manuscript text (which had stated a 7-day integration window) and the archived simulation code (which integrates Eq. 5 over 28 days) was identified and corrected in this version; all reported InSilico-pCR values (34.2%→91.5%) correspond to the 28-day window, with Day-7 IFP retained as an interim mechanistic checkpoint consistent with Fig. 3a. It assumes isotropic diffusion and omits spatial heterogeneity, three-dimensional vascular architecture and necrosis. Antibody and ADC molecular weights are treated as an approximate band—appropriate for a macro-scale transport argument but not for fine pharmacokinetics. The near-perfect convergence across agents partly reflects their genuinely narrow weight distribution and should be probed with engineered size variants (antibody fragments, larger conjugates). InSilico-pCR is a model output and has not been calibrated against measured pathological complete response. These caveats are reasons to test the idea, not to withhold it: the logic is simple, the intervention is cheap and safe, and the readout is a single tissue measurement.

4.5 Conclusion

A drug-agnostic digital twin predicts that elevated interstitial fluid pressure throttles IgG-scale oncology biologics as a class, and that telmisartan could decompress that barrier universally in NSCLC. The prediction is cheap to test, mechanistically grounded, and—if confirmed—reframes both systemic delivery (cardiology–oncology co-prescribing) and local therapy (InSilico-Guided Minimal Resection). We release the engine openly to invite falsification.

Tables

Table 1 | Macromolecular agents (IgG-scale, transport-limited). Approximate intact-antibody-scale values; all within ~145–153 kDa.

Agent	Target / class	MW (kDa)	Role
Amivantamab	EGFR/MET — bispecific antibody	~148	Reference macromolecule
Datopotamab deruxtecan	TROP2 — ADC	~152	Antibody scaffold ~148 kDa + payload
Trastuzumab deruxtecan	HER2 — ADC	~153	Approved in HER2-mutant NSCLC

Agent	Target / class	MW (kDa)	Role
Patritumab deruxtecan	HER3 — ADC	~153	Active after EGFR-TKI resistance
Pembrolizumab	PD-1 — checkpoint inhibitor	~149	Peritumoral access rate-limiting
Atezolizumab	PD-L1 — checkpoint inhibitor	~145	Compact IgG1 scaffold
Durvalumab	PD-L1 — checkpoint inhibitor	~149	Consolidation backbone
Bevacizumab	VEGF — anti-angiogenic	~149	Itself vascular-normalising
Ramucirumab	VEGFR2 — anti-angiogenic	~147	Modulates vascular permeability

Table 2 | Small-molecule agents (TKIs, transport-insensitive).

Agent	Target	MW (Da)
Osimertinib	EGFR	433
Lazertinib	EGFR	510
Alectinib	ALK	483
Lorlatinib	ALK/ROS1	406
Sotorasib	KRAS G12C	561
Selpercatinib	RET	526
Capmatinib	MET	412
Entrectinib	ROS1/NTRK	460

Declarations

Acknowledgements. Supported by JSPS KAKENHI Grant Number JP24K15840.

Competing interests. The author declares no competing interests.

Code and data availability. The drug database, engine source code (InSilico-K Universal) and analysis scripts that reproduce all figures and reported values are openly available under the MIT licence, archived on Zenodo (DOI 10.5281/zenodo.21123699) as a supplement to the originating preprint [8]; they are additionally provided as Supplementary Information.

Prior publication. This study extends the single-agent digital-twin platform previously deposited as a preprint [8]. No part of the present work has been published in a peer-reviewed journal.

Declaration of generative AI. The author used generative AI tools for structural organization, language refinement and coding assistance, reviewed and edited all content, and takes full responsibility for the publication.

References

1. Cho, B. C. et al. Amivantamab plus lazertinib in previously untreated EGFR-mutated advanced NSCLC (MARIPOSA). N. Engl. J. Med. 391, 1486–1498 (2024).

2. Moores, S. L. et al. A novel bispecific antibody targeting EGFR and cMet is effective against EGFR inhibitor-resistant lung tumours. Cancer Res. 76, 3942–3953 (2016).

3. Yang, J. C. H. et al. Overall survival with amivantamab–lazertinib in EGFR-mutated advanced NSCLC. N. Engl. J. Med. 393, 1681–1693 (2025).

4. Ahn, M. J. et al. Datopotamab deruxtecan versus docetaxel for previously treated advanced or metastatic non-small cell lung cancer: the randomized, open-label phase III TROPION-Lung01 study. J. Clin. Oncol. 43, 260–272 (2025).

5. Goto, K. et al. Trastuzumab deruxtecan in patients with HER2-mutant metastatic non-small-cell lung cancer: primary results from the randomized, phase II DESTINY-Lung02 trial. J. Clin. Oncol. 41, 4852–4863 (2023).

6. Yu, H. A. et al. HERTHENA-Lung01, a phase II trial of patritumab deruxtecan (HER3-DXd) in EGFR-mutated non-small-cell lung cancer after EGFR tyrosine kinase inhibitor therapy and platinum-based chemotherapy. J. Clin. Oncol. 41, 5363–5375 (2023).

7. Fu, Z., Li, S., Han, S., Shi, C. & Zhang, Y. Antibody drug conjugate: the “biological missile” for targeted cancer therapy. Signal Transduct. Target. Ther. 7, 93 (2022).

8. Shimada, J. InSilico-K digital twin platform for optimizing neoadjuvant regimens and surgical de-escalation in lung cancer. Research Square (preprint) https://doi.org/10.21203/rs.3.rs-10074451/v1 (2026).

9. Chauhan, V. P. et al. Angiotensin inhibition enhances drug delivery and potentiates chemotherapy by decompressing tumour blood vessels. Nat. Commun. 4, 2516 (2013).

10. Wadsworth, B. J. et al. Angiotensin II type 1 receptor blocker telmisartan inhibits the development of transient hypoxia and improves tumour response to radiation. Cancer Lett. 493, 31–40 (2020).

11. Stylianopoulos, T., Munn, L. L. & Jain, R. K. Reengineering the physical microenvironment of tumors to improve drug delivery and efficacy: from mathematical modeling to bench to bedside. Trends Cancer 4, 292–319 (2018).

12. Katsoulakis, E. et al. Digital twins for health: a scoping review. npj Digit. Med. 7, 77 (2024).

13. Abramson, J. et al. Accurate structure prediction of biomolecular interactions with AlphaFold 3. Nature 630, 493–500 (2024).

14. Benzekry, S. et al. Classical mathematical models for description and prediction of experimental tumor growth. PLoS Comput. Biol. 10, e1003800 (2014).

15. Norton, L. & Simon, R. Tumor size, sensitivity to therapy, and design of treatment schedules. Cancer Treat. Rep. 61, 1307–1317 (1977).

16. Bozic, I. et al. Evolutionary dynamics of cancer in response to targeted combination therapy. eLife 2, e00747 (2013).

17. Morice, M. C. et al. A randomized comparison of a sirolimus-eluting stent with a standard stent for coronary revascularization. N. Engl. J. Med. 346, 1773–1780 (2002).

18. Serruys, P. W. et al. Percutaneous coronary intervention versus coronary-artery bypass grafting for severe coronary artery disease. N. Engl. J. Med. 360, 961–972 (2009).

19. Saji, H. et al. Segmentectomy versus lobectomy in small-sized peripheral non-small-cell lung cancer (JCOG0802/WJOG4607L): a multicentre, open-label, phase 3, randomised, controlled, non-inferiority trial. Lancet 399, 1607–1617 (2022).

20. Altorki, N. et al. Lobar or sublobar resection for peripheral stage IA non-small-cell lung cancer (CALGB 140503). N. Engl. J. Med. 388, 489–498 (2023).

21. Ginsberg, R. J. & Rubinstein, L. V. Randomized trial of lobectomy versus limited resection for T1 N0 non-small cell lung cancer. Lung Cancer Study Group. Ann. Thorac. Surg. 60, 615–623 (1995).

22. Darling, G. E. et al. Randomized trial of mediastinal lymph node sampling versus complete lymphadenectomy during pulmonary resection in patients with N0 or N1 (less than hilar) non-small cell lung cancer: results of the ACOSOG Z0030 trial. J. Thorac. Cardiovasc. Surg. 141, 662–670 (2011).

23. He, J. et al. Neoadjuvant osimertinib for resectable EGFR-mutated non-small cell lung cancer (NeoADAURA). J. Clin. Oncol. 43, 2875–2887 (2025).

24. Yoshida, K. et al. Is conversion therapy possible in stage IV gastric cancer: the proposal of new biological categories of classification. Gastric Cancer 19, 329–338 (2016).

Supplementary Files

This is a list of supplementary files associated with this preprint. Click to download.

- InSilicoKUniversalv1.0.0zenodo.zip